

Direct Band Gap Silicon Allotropes

Qianqian Wang,^{†,⊥} Bo Xu,^{†,⊥} Jian Sun,^{§,⊥} Hanyu Liu,[‡] Zhisheng Zhao,^{||} Dongli Yu,[†] Changzeng Fan,[†] and Julong He^{*,†}

[†]State Key Laboratory of Metastable Materials Science and Technology, Yanshan University, Qinhuangdao 066004, Hebei Province, China

[§]Department of Physics and National Laboratory of Solid State Microstructures, Nanjing University, Nanjing 210093, China

[‡]Department of Physics and Engineering Physics, University of Saskatchewan, Saskatchewan, Canada, S7N 5E2

^{||}Geophysical Laboratory, Carnegie Institution of Washington, Washington, DC 20015, United States

S Supporting Information

ABSTRACT: Elemental silicon has a large impact on the economy of the modern world and is of fundamental importance in the technological field, particularly in solar cell industry. The great demand of society for new clean energy and the shortcomings of the current silicon solar cells are calling for new materials that can make full use of the solar power. In this paper, six metastable allotropes of silicon with direct or quasidirect band gaps of 0.39–1.25 eV are predicted by *ab initio* calculations at ambient pressure. Five of them possess band gaps within the optimal range for high converting efficiency from solar energy to electric power and also have better optical properties than the Si-I phase. These Si structures with different band gaps could be applied to multiple p–n junction photovoltaic modules.

Due to the decreasing resource of fossil fuel and demand of reducing the carbon emission during the energy production, exploration of new clean energy is of great interest and fundamental importance. Converting sunlight into electricity through solar cells is considered to be one of the most promising technologies.¹ Because of the stability, durability, abundance, and nontoxicity, silicon (Si) solar cells using monocrystalline, polycrystalline, or amorphous Si in the form of wafers or thin-films still dominate the current photovoltaic market share.^{1d} Although the current silicon solar cell materials have numerous advantages, their shortcomings cannot be ignored. For instance, the indirect fundamental band gap (1.1 eV) in Si-I phase² leads to the absorption of photons needing the help of phonons. In addition, the direct optical gap of Si is larger than 3 eV, with little overlap with the solar spectral irradiance for AM1.5.^{2,3} These factors result in the low efficient absorption of the sunlight.

According to the Shockley–Queisser limit, the maximum theoretical solar converting efficiency of single p–n junction cells is a function of the band gap of materials, with a maximum of 33.7% solar energy that can be employed near a band gap of 1.34 eV.⁴ However, the commercial silicon cells can reach only 15–20%,⁵ which primarily results from the large energy difference between the direct and indirect gaps. To increase the performance of silicon solar cells, it would be helpful to

pursue new direct band gap silicon allotropes with band gaps around the optimum value of the solar converting efficiency. Si can have a direct band gap through fabricating low-dimensional Si structures, such as highly porous Si, Si quantum wires, Si quantum dots. For example, visible light emission was observed in highly porous Si, which is composed of arrays of linear quantum wires.⁶ Theoretical investigations on low-dimensional silicon indicated direct, optically allowed band gaps.⁷ Another way to achieve direct band gap is exploring silicon with new crystal structures. Recently, Botti et al.⁸ presented a number of low-energy silicon allotropes with quasidirect band gaps between 1 and 1.5 eV. Subsequently, Xiang et al. proposed a cubic Si₂₀-T phase with a quasidirect gap of 1.55 eV.⁹ These phases are predicted to exhibit better optical properties than diamond Si. These exciting works would encourage further exploration of new silicon structures with direct band gaps.

However, even though the band gap of a silicon solar cell is located in the optimal value and reaches the maximum conversion efficiency, a single-junction cell cannot absorb the whole solar spectrum. For example, the solar energy with frequencies below or far above the band gap could not be fully utilized. To further enhance the efficiency of silicon solar cell, a useful way is to use the stacked tandem structure. Tandem cells require semiconductors with different band gaps tuning specific frequencies of the solar spectrum. The sunlight in different wavelengths could be absorbed by corresponding photoactive layers. Under unconcentrated sunlight, tandem solar cells with an infinite number of p–n junctions can convert a maximum of 68% of the solar energy,¹⁰ which breaks the Shockley–Queisser limit. Therefore, silicon materials with different direct band gaps are desired to take full advantage of sunlight.

Silicon is known to exist in a variety of allotropes, including the most stable cubic diamond silicon (Si-I) and several metastable silicon allotropes. Metastable BC8-structured Si-III¹¹ and/or R8-structured Si-XII¹² could be quenched to ambient pressure by decompressing the high-pressure phase, β -Sn structured Si-II. The lonsdaleite phase¹¹ as well as Si-XIII¹³ (resolved as the T12 structure, ref 14) can be formed by annealing BC8 and/or R8 phase at ambient pressure. However, the R8 phase, T12-Si and lonsdaleite phase all show indirect

Received: April 10, 2014

Published: June 27, 2014

band gaps, while the BC8 silicon is a semimetal.^{14,15} Also, rapid pressure release of Si-II can produce metastable tetragonal phases of Si-VIII and Si-IX (crystal structures unresolved).¹⁶ The guest-free Si₁₃₆, prepared by thermal decomposition of alkaline metal silicides with subsequent chemical treatment, was reported to possess a large direct band gap of ca. 1.9 eV.¹⁷ Hence, identification of silicon structures with variable direct band gaps is crucial for both scientific and applicational reasons.

In this paper, six silicon structures with direct or quasidirect band gaps ranging from 0.39 to 1.25 eV have been revealed using particle swarm optimization (PSO) algorithm. All the six structures are energetically favorable than the Si₂₀-T phase at ambient pressure.⁹ In addition, they exhibit better optical properties than that of Si-I. If these proposed metastable structures can be synthesized, they can be applied in single p–n junction thin-film solar cells or tandem photovoltaic devices.

Structure searches were carried out at zero pressure with simulation cell of up to 30 atoms using CALYPSO, which was unbiased by any known structure information.¹⁸ The structural relaxations were performed using density functional theory (DFT) with the Perdew–Burke–Ernzerh (PBE) generalized gradient approximation,¹⁹ as implemented in the VASP code.²⁰ The dynamic stability of the structures was verified by the phonon spectrum calculation through the direct supercell method as implemented in the PHONOPY code.²¹ Both PBE functional and Heyd–Scuseria–Ernzerhof (HSE) hybrid functional²² were employed to calculate the properties of investigated Si structures, such as elastic modulus, electronic, and optical properties. See Supporting Information (SI) for more details.

The crystal structures of six metastable silicon allotropes with direct or quasidirect band gap are shown in Figure 1. The lattice

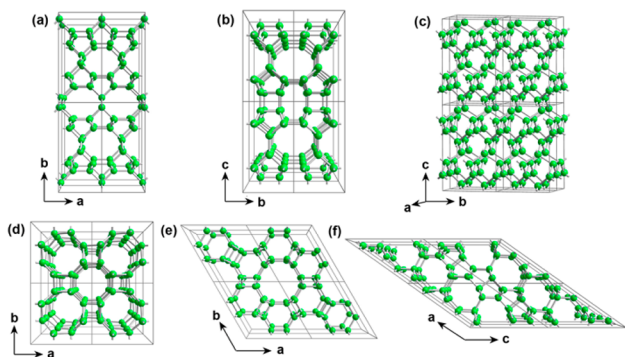


Figure 1. Crystal structures of (a) oC12-Si, (b) tP16-Si, (c) oF16-Si, (d) tI16-Si, (e) hP12-Si, and (f) mC12-Si.

parameters of these structures are listed in the Table S1. All structures are four-coordinated with different degrees of distortion. Except oF16-Si, all structures contain one-dimensional (oC12-Si, tI16-Si, hP12-Si, and mC12-Si) or two-dimensional (tP16-Si) tunnel-like voids joined by four-, five-, or six-membered rings. oC12-Si and mC12-Si share some structural similarity: both are composed of five-, six-, and eight-membered rings with different stacking styles. tI16-Si and hP12-Si are composed of (4, 0) and (3, 3) silicon nanotubes bonding with each other into a three-dimensional framework, respectively. Therefore, tI16-Si and hP12-Si can also be called 3D-(4, 0)-Si and 3D-(3, 3)-Si, respectively. The oF16-Si is different from the others for its structural resemblance to Si-I phase.

To examine the thermodynamic stability, the enthalpies of proposed structures were compared with the experimentally known Si-I and Si-II and the theoretically proposed Si₂₀-T, as depicted in Figure 2. Si-I remains as the most stable phase at

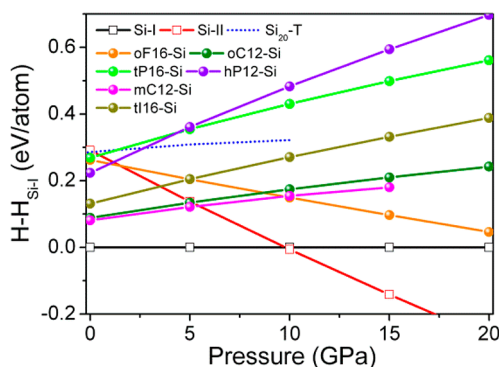


Figure 2. Calculated enthalpies of different silicon structures relative to the Si-I as a function of pressure.

zero pressure. All newly predicted structures are energetically more favorable than Si₂₀-T phase⁹ at zero pressure. The energy sequence of the six proposed Si phases from low to high is mC12-Si, oC12-Si, tI16-Si, hP12-Si, oF16-Si, and tP16-Si. Among them, the most unfavorable tP16-Si is higher in energy than Si-I by 0.269 eV/atom at zero pressure, but lower than that of Si₂₀-T by 0.017 eV/atom, while the most stable mC12-Si is 0.205 eV/atom lower than Si₂₀-T. Generally, distortion of the tetrahedron in these metastable structures leads to their higher energy. The planar four-membered rings will result in more severe distortion than five-membered rings. Therefore, mC12-Si and oC12-Si gain lower energy at zero pressure because of the exclusion of four-membered rings in the structures. It is noted that tI16-Si containing four-membered rings but has lower energy than hP12-Si and tP16-Si. The reason is that the four-membered rings in tI16-Si are not planar, thus the distortion in tI16-Si is not as much as those in hP12-Si and tP16-Si. The dynamic stability of these structures was verified by the phonon spectrum calculations, which show no imaginary frequency along the whole Brillouin zone (Figure S1).

Enthalpy represents the free energy of a system at zero temperature. For real applications in solar cells, these structures should endure room temperature or even higher temperature. The effect of finite temperature should be considered by including the contribution of entropy. The free energies of those structures were calculated from 0 to 1000 K at ambient pressure, as shown in Figure S2. The energy sequence of these structures does not change with increased temperature, and the free energies of our proposed structures stay below that of Si₂₀-T.⁹ To identify whether atoms in the proposed structures will move away from the original lattice sites at high temperature, the position correlation functions of the six structures were simulated with molecular dynamics calculations (Figures S3 and S4). All structures except oF16-Si are stable at 1000 K. oF16-Si is stable at 300 K, however, it became unstable at higher temperature.

The diamond-like oF16-Si (2.52 g/cm³) is denser than the Si-I phase. Other phases with tunnel-like voids show low densities comparable to that of the silicon clathrate.²³ hP12-Si, possessing the largest voids of the (3, 3) tubes, has the lowest density of 1.85 g/cm³. Due to the structural similarity and smaller tunnel voids, oC12-Si and the mC12-Si have almost the

same density, but denser than the hP12-Si, tP16-Si, and tI16-Si that have larger tunnel voids. Another feature of the porous structure is the reduction of the bulk and shear moduli, owing to the lower bond density and valence electrons density (Table 1). The most porous structures of the proposed structures are

Table 1. Band Gap E_g (eV), Bulk Modulus B (GPa), and Shear Modulus G (GPa) of the Proposed Silicon Structures and Si-I Phase^a

crystal	E_g		type	B		G	
	PBE	HSE		PBE	HSE	PBE	HSE
Si-I	0.66	1.20	ID	94	93	67	67
hP12-Si	0.02	0.39	QD	68	68	37	39
oF16-Si	0.33	0.81	D	96	95	67	69
tP16-Si	0.33	0.91	D	74	73	34	36
oC12-Si	0.43	0.96	QD	83	81	58	59
mC12-Si	0.64	1.24	D	80	81	53	55
tI16-Si	0.62	1.25	D	80	79	46	47

^aID, QD, and D represent indirect, quasidirect, and direct band gaps, respectively.

tP16-Si and hP12-Si, and they demonstrate the lowest bulk and shear moduli. However, tI16-Si shows comparable density with that of tP16-Si but has much higher values of bulk and shear moduli. This could be attributed to the stronger bond strength caused by the less distortion in the tI16-Si structure. The densest oF16-Si demonstrates the highest bulk and shear moduli, which are almost the same as those of Si-I.

For materials used in photovoltaic devices, the band gap is a critical parameter because the conversion efficient from sunlight into electrical power is a function of the band gap.⁴ We calculated the electronic band structures of the newly predicted structures with both PBE and HSE06 functionals.^{19,22} The band gaps of different structures are listed in Table 1. Within the PBE functional, our calculation indicates that the band gap of oC12-Si is quasidirect (with a very small energy difference of 0.0007 eV between the direct and fundamental band gaps), and band gaps of all the other structures are direct. It is well-known that the Kohn–Sham DFT usually underestimates the band gaps, which is confirmed in our calculations (see Table 1). Figure 3 demonstrates the electronic band structures calculated with HSE06 hybrid functional. oF16-Si, tP16-Si, mC12-Si, and tI16-Si phases show direct band gaps, where the conduction band minimum and valence band maximum are located at the G, G, M, and Z points in the Brillouin zone, respectively. hP12-Si and oC12-Si show quasidirect band gaps since the conduction band minimum and valence band maximum are not at the same k point in the Brillouin zone. For hP12-Si, the conduction band minimum is at $(-0.037, 0.074, 0.0)$ point along the K–G direction, and the valence band maximum is at the G point. For oC12-Si, the conduction band minimum is at the Y point, and the valence band maximum is at the G point. The energy differences between the direct and fundamental band gaps are only 0.016 and 0.0062 eV for hP12-Si and oC12-Si, respectively. We note that tI16-Si and mC12-Si have the largest band gap of 1.25 and 1.24 eV, respectively. Band gaps of these structures (except hP12-Si) fall into the optimum value range as suggested by the Shockley–Queisser limit.

Imaginary parts of dielectric functions and the absorption spectra of these structures were calculated employing the HSE06 functional to estimate their optical properties (Figure 4). The imaginary parts of dielectric functions of Si-I are also

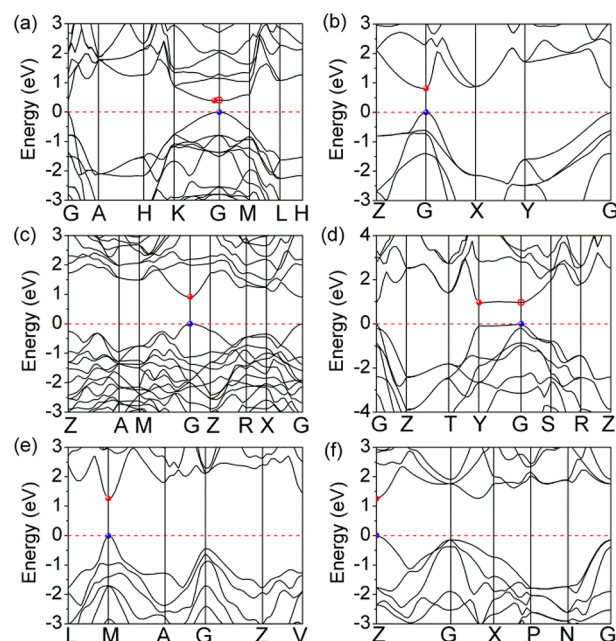


Figure 3. Band structures of (a) hP12-Si, (b) oF16-Si, (c) tP16-Si, (d) oC12-Si, (e) mC12-Si, and (f) tI16-Si calculated with HSE06 functional. The red and blue points indicate the conduction band minimum and valence band maximum, respectively. The red circles in (a) and (d) emphasize the direct band gaps in hP12-Si and oC12-Si structures.

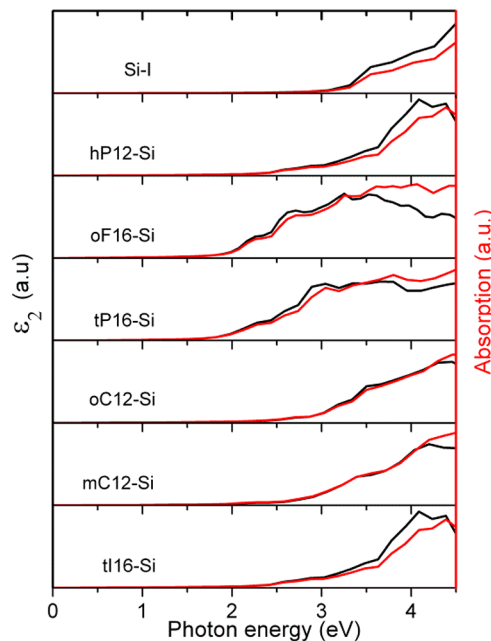


Figure 4. Imaginary part of dielectric function and optical absorption coefficient for different structures compared with that of Si-I phase calculated within HSE06 functional.

calculated for comparison. It is known that the low conversion efficiency of Si-I is partly due to its large optical gap leading to a waste of solar energy below the optical gap energy. The present results suggest our proposed allotropes start to absorb the sunlight at lower energies than that of Si-I. The absorption of these allotropes starts at different energies that cover a variety of frequencies in the solar spectrum. Therefore, a combination of these phases would capture more sunlight. Highly efficient

solar devices could be fabricated by stacking these phases in series.

In fact, it is more important to investigate the possibility of experimental synthesis of these structures. Previous works indicated that high-energy structures can be accessed by using a high-energy precursor or chemical synthesis methods, such as the Cco-C8 from compressing carbon nanotube bundles,²⁴ and silicon clathrates from thermal decomposition of alkaline metal silicides.^{17a,23} Among the six predicted metastable phases, oF16-Si with high density is pressure driven and has a lower energy than Si-II at ambient pressure, which may probably be obtained by quenching Si-II phase with controlled unloading rate and temperature.¹⁶ The other five phases with much lower densities might be synthesized with chemical methods similar to that of silicon clathrates.^{17a,23,25} The recent chemical preparation of m-allo-Ge also suggested the diversity of group-IV elements and the possible routes to realize them.²⁶ It is noted that tI16-Si and hP12-Si may be realized by compressing (4, 0) and (3, 3) silicon nanotube bundles, respectively.

In summary, six metastable silicon allotropes with direct or quasidirect band gaps are revealed using crystal structure searches combined with *ab initio* calculations. These structures are four-coordinated with different degrees of distortion and energetically superior to the recently proposed Si₂₀-T. Five of the predicted structures possess variable band gaps in the range of optimal gap value for achieving high converting efficiency of solar energy into electric power. These structures can absorb sunlight with different frequencies, providing appealing features for application in the tandem multijunction photovoltaic modules.

■ ASSOCIATED CONTENT

● Supporting Information

Calculation details, crystal structure information, and phonon dispersion curves, position correlation functions from molecular dynamics calculation, POSCAR files. This material is available free of charge via the Internet at <http://pubs.acs.org>.

■ AUTHOR INFORMATION

Corresponding Author

hjl@ysu.edu.cn

Author Contributions

[†]These authors contributed equally.

Notes

The authors declare no competing financial interest.

■ ACKNOWLEDGMENTS

This work was supported by NBRPC (grant no. 2011CB808205), NSFC (grant nos. 51121061, 91022029, 51272227, and 51372112), and by the Science Foundation of Yanshan University for the Excellent Ph.D. Students (grant no. YSUSF201201). Z.Z.'s fellowship is supported by the grant of Carnegie Institution of Washington and Energy Frontier Research in Extreme Environments Center (EFree) funded by the U.S. Department of Energy, Office of Science under award no. DE-SC0001057.

■ REFERENCES

(1) (a) Green, M. A. *Sol. Energy* **2003**, *74*, 181. (b) Kazmerski, L. L. *J. Electron Spectrosc. Relat. Phenom.* **2006**, *150*, 105. (c) Braga, A. F. B.; Moreira, S. P.; Zampieri, P. R.; Bacchin, J. M. G.; Mei, P. R. *Sol. Energy*

Mater. Sol. Cells **2008**, *92*, 418. (d) Petter Jelle, B.; Breivik, C.; Drolsum Røkenes, H. *Sol. Energy Mater. Sol. Cells* **2012**, *100*, 69.

- (2) Hybertsen, M.; Louie, S. *Phys. Rev. Lett.* **1985**, *55*, 1418.
(3) Malone, B. D.; Louie, S. G.; Cohen, M. L. *Phys. Rev. B* **2010**, *81*, 115201.
(4) Shockley, W.; Queisser, H. J. *J. Appl. Phys.* **1961**, *32*, 510.
(5) Service, R. F. *Science* **2008**, *319*, 718.
(6) Cullis, A. G.; Canham, L. T. *Nature* **1991**, *353*, 335.
(7) (a) Ohno, T.; Shiraishi, K.; Ogawa, T. *Phys. Rev. Lett.* **1992**, *69*, 2400. (b) Delley, B.; Steigmeier, E. *Phys. Rev. B* **1993**, *47*, 1397.
(8) Botti, S.; Flores-Livas, J.; Amsler, M.; Goedecker, S.; Marques, M. *Phys. Rev. B* **2012**, *86*, 121204.
(9) Xiang, H. J.; Huang, B.; Kan, E.; Wei, S.-H.; Gong, X. G. *Phys. Rev. Lett.* **2013**, *110*, 118702.
(10) Vos, A. D. *J. Phys. D: Appl. Phys.* **1980**, *13*, 839.
(11) Wentorf, R. H.; a, J.; K, J. S. *Science* **1963**, *139*, 338.
(12) Crain, J.; Ackland, G.; Maclean, J.; Piltz, R.; Hatton, P.; Pawley, G. *Phys. Rev. B* **1994**, *50*, 13043.
(13) (a) Dornich, V.; Gogotsi, Y. *Rev. Adv. Mater. Sci.* **2002**, *3*, 1. (b) Ge, D. *J. Appl. Phys.* **2004**, *95*, 2725. (c) Ruffell, S.; Haberl, B.; Koenig, S.; Bradby, J. E.; Williams, J. S. *J. Appl. Phys.* **2009**, *105*, 093513.
(14) Zhao, Z.; Tian, F.; Dong, X.; Li, Q.; Wang, Q.; Wang, H.; Zhong, X.; Xu, B.; Yu, D.; He, J.; Wang, H.-T.; Ma, Y.; Tian, Y. *J. Am. Chem. Soc.* **2012**, *134*, 12362.
(15) Malone, B.; Sau, J.; Cohen, M. *Phys. Rev. B* **2008**, *78*, 035210.
(16) Zhao, Y.-X.; Buehler, F.; Sites, J. R.; Spain, I. L. *Solid State Commun.* **1986**, *59*, 679.
(17) (a) Gryko, J.; McMillan, P. F.; Marzke, R. F.; Ramachandran, G. K.; Patton, D.; Deb, S. K.; Sankey, O. F. *Phys. Rev. B* **2000**, *62*, R7707. (b) Blase, X. *Phys. Rev. B* **2003**, *67*, 035211.
(18) (a) Wang, Y.; Lv, J.; Zhu, L.; Ma, Y. *Phys. Rev. B* **2010**, *82*, 094116. (b) Wang, Y.; Lv, J.; Zhu, L.; Ma, Y. *Comput. Phys. Commun.* **2012**, *183*, 2063.
(19) Perdew, J. P.; Burke, K.; Ernzerhof, M. *Phys. Rev. Lett.* **1996**, *77*, 3865.
(20) Kresse, G.; Furthmüller, J. *Phys. Rev. B* **1996**, *54*, 11169.
(21) Togo, A.; Oba, F.; Tanaka, I. *Phys. Rev. B* **2008**, *78*, 134106.
(22) Heyd, J.; Scuseria, G. E.; Ernzerhof, M. *J. Chem. Phys.* **2003**, *118*, 8207.
(23) Ramachandran, G. K.; Dong, J.; Diefenbacher, J.; Gryko, J.; Marzke, R. F.; Sankey, O. F.; McMillan, P. F. *J. Solid State Chem.* **1999**, *145*, 716.
(24) Zhao, Z.; Xu, B.; Zhou, X.-F.; Wang, L.-M.; Wen, B.; He, J.; Liu, Z.; Wang, H.-T.; Tian, Y. *Phys. Rev. Lett.* **2011**, *107*, 215502.
(25) Kasper, J. S.; Hagenmuller, P.; Pouchard, M.; Cros, C. *Science* **1965**, *150*, 1713.
(26) (a) Kiefer, F.; Karttunen, A. J.; Döblinger, M.; Fässler, T. F. *Chem. Mater.* **2011**, *23*, 4578. (b) Zaikina, J. V.; Muthuswamy, E.; Lilova, K. L.; Gibbs, Z. M.; Zeilinger, M.; Snyder, G. J.; Fässler, T. F.; Navrotsky, A.; Kauzlarich, S. M. *Chem. Mater.* **2014**, *26*, 3263.